

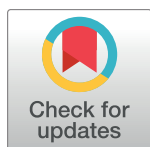
RESEARCH ARTICLE

# Essential multimeric enzymes in kinetoplastid parasites: A host of potentially druggable protein-protein interactions

Leah M. Wachsmuth, Meredith G. Johnson, Jason Gavenonis\*

Department of Chemistry, Dickinson College, Carlisle, Pennsylvania, United States of America

\* [gavenonj@dickinson.edu](mailto:gavenonj@dickinson.edu)



## Abstract

Parasitic diseases caused by kinetoplastid parasites of the genera *Trypanosoma* and *Leishmania* are an urgent public health crisis in the developing world. These closely related species possess a number of multimeric enzymes in highly conserved pathways involved in vital functions, such as redox homeostasis and nucleotide synthesis. Computational alanine scanning of these protein-protein interfaces has revealed a host of potentially ligandable sites on several established and emerging anti-parasitic drug targets. Analysis of interfaces with multiple clustered hotspots has suggested several potentially inhibitable protein-protein interactions that may have been overlooked by previous large-scale analyses focusing solely on secondary structure. These protein-protein interactions provide a promising lead for the development of new peptide and macrocycle inhibitors of these enzymes.

## OPEN ACCESS

**Citation:** Wachsmuth LM, Johnson MG, Gavenonis J (2017) Essential multimeric enzymes in kinetoplastid parasites: A host of potentially druggable protein-protein interactions. *PLoS Negl Trop Dis* 11(6): e0005720. <https://doi.org/10.1371/journal.pntd.0005720>

**Editor:** Timothy G. Geary, McGill University, CANADA

**Received:** February 13, 2017

**Accepted:** June 16, 2017

**Published:** June 29, 2017

**Copyright:** © 2017 Wachsmuth et al. This is an open access article distributed under the terms of the [Creative Commons Attribution License](https://creativecommons.org/licenses/by/4.0/), which permits unrestricted use, distribution, and reproduction in any medium, provided the original author and source are credited.

**Data Availability Statement:** All relevant data are within the paper and its Supporting Information files.

**Funding:** JG and LMW were supported in part by The Robert D. and Barbara C. Crouch Student Faculty Research Fund at Dickinson College. The funders had no role in study design, data collection and analysis, decision to publish, or preparation of the manuscript.

**Competing interests:** The authors have declared that no competing interests exist.

## Author summary

Neglected tropical diseases caused by parasites of the genera *Trypanosoma* and *Leishmania* affect millions of people, primarily in the developing world. Due to a historical lack of incentive or interest, few new drugs have been developed to treat these conditions. Numerous efforts have targeted the metabolism of trypanothione, an essential molecule for maintaining the redox homeostasis of these parasites. This study uses freely available structural databases and computational tools to identify new druggable sites on several essential proteins in these organisms by disrupting the protein-protein interactions that allow multimeric enzymes to function. Five of the targets identified in this study are involved in redox homeostasis, while the remainder are involved in other essential metabolic or biosynthetic processes. Nine have been identified in other computational databases, and two have already been experimentally verified, which suggests that protein-protein interaction inhibition of multimeric enzymes may be a general and viable route for the development of new trypanocidal agents.

## Introduction

Infections caused by the kinetoplastid parasites *Leishmania spp.*, *Trypanosoma brucei*, and *Trypanosoma cruzi* are estimated collectively to put at risk one billion people, resulting in tens of millions of infections and upwards of ten thousand deaths per year [1]. Neglected tropical diseases (NTDs) caused by these parasites primarily occur in the developing world and are infrequently the target of commercial drug-development efforts [2]. A number of highly conserved enzymes are present across these pathogenic species, despite substantial genomic diversity [3]. Furthermore, the proliferation of high-resolution crystallographic data affords the opportunity to identify new mechanisms for inhibiting both established and emerging drug targets in these organisms. Recent drug-repurposing efforts have allowed for the development of promising new leads based on previous work on homologous targets, such as kinases and heat-shock proteins, in human diseases [4,5].

Just as neglected tropical diseases have received comparatively little attention from the drug discovery community, so too have protein-protein interactions (PPIs), which are characterized by larger surface area and lower binding affinity than is typical for drug-like molecules [6,7]. A substantial fraction of the protein-protein interaction energy is localized in a few amino acid residues, known as “hot spots,” which are often surface-exposed hydrophobic amino acid residues [8]. Computational alanine scanning can generally predict these interface hot spots with a 79% success rate [9]. This has led to the successful development of several inhibitors of PPIs [10–12]. Of greatest relevance to NTDs, this approach has been applied to inhibition of the cysteine protease cruzain, based on the interaction with its native inhibitor chagasin [13]. Targeting PPIs of multimeric enzymes [14,15] in these pathogens, by avoiding the highly conserved substrate-binding domains, should allow for fine-tuning selectivity to avoid inhibition of the homologous host enzymes [15]. This approach has been successful in PPI-based inhibition of the homodimeric enzyme, triosephosphate isomerase (TIM), in *P. falciparum* [14] and *T. cruzi* [16]. Thus, a systematic analysis of these overlooked targets for neglected diseases may reveal both new drug targets and new approaches to inhibit well-established targets.

## Methods

Structures of multi-protein complexes from the family Trypanosomatidae were obtained using the advanced search functionality of the Protein Data Bank [17]. Structures with  $>4$  Å resolution or  $>90\%$  similarity were excluded. The PDB files were cleaned to remove headers, retaining only ATOM line entries, using a shell script. Computational alanine scanning [9] was performed using Rosetta 3.6 and PyRosetta [18], with a modified version of the alanine-scanning script originally developed by the Gray lab [19]. The updated Talaris2013 scorefunction [20] was parameterized to match an established general protocol [9,21] without environment-dependent hydrogen bonding terms. Default score function weights were retained, but line 129 of the script was replaced as follows to implement these changes:

```
scorefxn = create_score_function('talaris2013')
```

Interfaces that were determined to have at least three hot spots ( $\Delta\Delta G \geq 1.0$  Rosetta Energy Units (REU), average of 20 scans, 8.0 Å interface cutoff) by this method were further examined for proximity of the hot spots in both primary [22] sequence and secondary/tertiary structure. Complexes with at least two hot spots in close proximity were cross-checked for presence in existing databases of helix [23,24] and loop [25,26] interaction motifs, then with existing literature for experimentally verified interface hot spots, and finally for identity as an established or emerging drug target [27–31]. Amino acid residues falling just below the threshold ( $\Delta\Delta G$  between 0.8 and 1.0 REU) were also considered when proximal to multiple interface hot spots.

During the preparation of this manuscript, the authors became aware of the Peptiderive server [32], which allows for the rapid examination of single PPI interfaces for hot-spot rich segments of a defined length. The PPIs identified in this study were subsequently re-examined using Peptiderive to locate decameric “hot segments” for comparison.

## Results and discussion

### Identification and characterization of PPIs

Of the 1,076 kinetoplastid protein structures deposited in the PDB, 207 are multi-chain biological assemblies. Computational alanine scanning identifies 56 structures containing at least three putative interface hot spots (27%). Hot spots are defined as any amino acid residue that, when mutated to alanine, increased the  $\Delta\Delta G_{\text{complex}}$  by at least 1.0 REU [33], a threshold that generally has a 79% correspondence with experimentally observed hot spots [9]. Among these 56 structures, 46 contain multiple hot spots on the same helix (27) or loop (19). Despite the 90% sequence identity cutoff, several homologous proteins from *Leishmania spp.*, *Trypanosoma spp.*, and the non-pathogenic model organism *Crithidia fasciculata* appear multiple times (*vide infra*), reducing the number of unique interfaces to 34. Analysis of these 34 complexes reveals 12 unique PPIs that are either established drug targets in *T. cruzi*, *T. brucei*, or *Leishmania spp.* or essential enzymes and structurally or functionally obligate multimers. Drug targets with inhibitable PPIs, their potentially inhibitory peptide sequences, and a comparison to HippDB, Loopfinder, Peptiderive, and experimental results are listed in Table 1.

### Trypanothione metabolism and the pentose phosphate pathway

Five targets are involved in the redox metabolism of trypanothione, an essential pathway for the parasites’ antioxidant defense that has been the target of numerous drug development

**Table 1. Potential self-inhibitory peptides from multimeric enzymes in kinetoplastid parasites.**

Target	Species	Peptide	Helix	Loop	Segment	Assay
TryR	<i>Cf</i>	71-TIRESAGFGWELD	+	++	++	+ [34]
GS	<i>Tb</i>	2-VLKLLLEL	+	+	+	
TXNPx	<i>Lm</i>	145-NDMPVGR	+	++	++	
G6PDH	<i>Tc</i>	441-AMYLKLTAKTPGLLNDTHQTEL	+	+	+	++ [35]
6PGDH	<i>Tb</i>	251-LTEHVMDRI	+	+	+	
RpiB	<i>Tc</i>	141-RIEKIRAIEASH	++	+	++	
GalE	<i>Tb</i>	111-PLKYDNNVVGILRLL	++	++	++	
FPPS	<i>Tb</i>	25-FDMDPNRVRYL	+	+	++	
TAT	<i>Tc</i>	54-AQIKKLKEAIDS	+	--	++	
PTR1	<i>Lm</i>	192-TIYTMKGALEGLTRSAALELA	++	+	++	
dUTPase	<i>Lm</i>	51-ELLDSYPWKWWK	+	--	++	
DHODH	<i>Lm</i>	201-VIDAETESVVIKPKQGF	--	++	++	

Targets for the 12 potentially self-inhibitory peptides identified in this study, organism in which they are found, peptide sequences, and comparison to previous approaches relying on helical secondary structure (HippDB, “Helix”) or loops amenable to cyclization (Loopfinder, “Loop”), identification of decameric hot segments (Peptiderive “Segment”), and experimentally validated *in vitro* enzyme inhibitors (“Assay”). Full sequences and scores for peptides identified in HippDB, Loopfinder, and using the Peptiderive Server can be found in S1 Table. *Cf*: *Crithidia fasciculata*; *Tb*: *Trypanosoma brucei*; *Tc*: *Trypanosoma cruzi*; *Lm*: *Leishmania major*.

+ non-overlapping peptide sequence

++ overlapping sequence

--not found in database

<https://doi.org/10.1371/journal.pntd.0005720.t001>

efforts [36]. Central to this pathway is Trypanothione reductase (TryR), an essential enzyme which maintains trypanothione, T(SH)<sub>2</sub>, in the reduced state. T(SH)<sub>2</sub> is produced from glutathione (GSH), which is both synthesized *de novo* by glutathione synthetase (GS) and scavenged extracellularly from the host. TryR utilizes NADPH as a reductant, produced primarily from the pentose phosphate pathway (PPP) by glucose 6-phosphate dehydrogenase (G6PDH), which itself is induced by the presence of hydrogen peroxide, and 6-phosphogluconate dehydrogenase (6PGDH) [37]. Several enzymes use T(SH)<sub>2</sub> to detoxify specific reactive oxygen species, including trypanredoxin peroxidase (TXNPx), which reduces hydroperoxides produced by the host's immune response.

Trypanothione reductase is a well-established drug target, with almost all known inhibitors targeting the active site through covalent inactivation of the catalytic cysteine residues or binding of polycationic species in the active site [2,30,38,39]. Recent computational and experimental studies have identified a hot-spot-containing helix in *L. infantum* TryR that inhibits TS<sub>2</sub> reduction by disrupting dimerization of the enzyme, as demonstrated by kinetics and ELISA [34,40]. This helix overlaps, but shares little sequence homology with, a helix that disrupts dimerization of human glutathione reductase (hGR), although it presents a strikingly similar helical face (S1 Fig). The hGR peptide prevents refolding of denatured hGR, but does not inhibit the activity of the native enzyme [41], minimizing the possibility of hGR inhibition from an isosteric TryR inhibitor. Beyond this known mode of inhibition, this study identified a short helix-breaking loop in *C. fasciculata* (Fig 1A), *T. brucei*, *T. cruzi*, and *L. infantum* TryR containing three hotspots, Ile-72, Phe-78, and Leu-82, which matches a loop in *Li*TryR identified by Loopfinder (heat score: 3), overlaps a segment predicted by Peptiderive (22% interface energy), and contains one hotspot (Trp-80) that has been verified experimentally (Fig 1) [34]. This proposed inhibitory peptide is predicted to contribute more to the interface energy than the established helix-based inhibitor.

Glutathione synthetase is the second step in *de novo* synthesis of TS<sub>2</sub>, producing glutathione from  $\gamma$ -glutamylcysteine, glycine, and ATP. Knockout of GS in *T. brucei* results in a growth-restriction phenotype that is not rescued by addition of exogenous glutathione, suggesting that GS may be druggable [43]. Initial structural characterization of *T. brucei* GS had suggested that the high homology in the regions involved in substrate and cofactor binding and catalysis would make GS a suboptimal drug target [44]. However, the helix identified in this study differs greatly from the human homolog in both primary sequence and secondary structure. While the proposed inhibitory sequence, 2-VLKLLLEL, contains only two putative hot spots, Leu-3 and Leu-7, recombinant *Tb*GS with an N-terminal His<sub>6</sub> tag has drastically reduced catalytic turnover [45], suggesting the importance of the N-terminus in dimerization and providing a plausible route to selective PPI-based inhibition of *Tb*GS in this region. Both HippDB (17%) and Peptiderive (22%) identified segments near the N-terminus predicted to contribute substantially to the stability of the PPI.

Trypanredoxin peroxidase catalyzes the TS<sub>2</sub>-dependant detoxification of peroxides, is an essential enzyme in *T. brucei* and *L. major*, and has been proposed as a potential drug target due to the constitutively high levels of peroxide, especially in *T. brucei* [46–50]. TXNPx is an obligate homodimer, with catalytic cysteine residues for a single active site located on both subunits [48]. This study identifies an unstructured loop containing three hot spots, Asn-145, Val-149, and Arg-151, in *L. major*, *T. brucei*, and *C. fasciculata* (Ile-149) in a hydrophobic cleft on the surface. This peptide matches a loop identified by Loopfinder (heat score: 9) and a segment identified by Peptiderive (27% interface energy). HippDB contains one short, two-turn helix, predicted to contribute only 9% interface energy (Fig 1).

Glucose-6-phosphate dehydrogenase catalyzes the first reaction in the pentose phosphate pathway, oxidizing glucose-6-phosphate to 6-phosphogluconolactone and producing NADPH



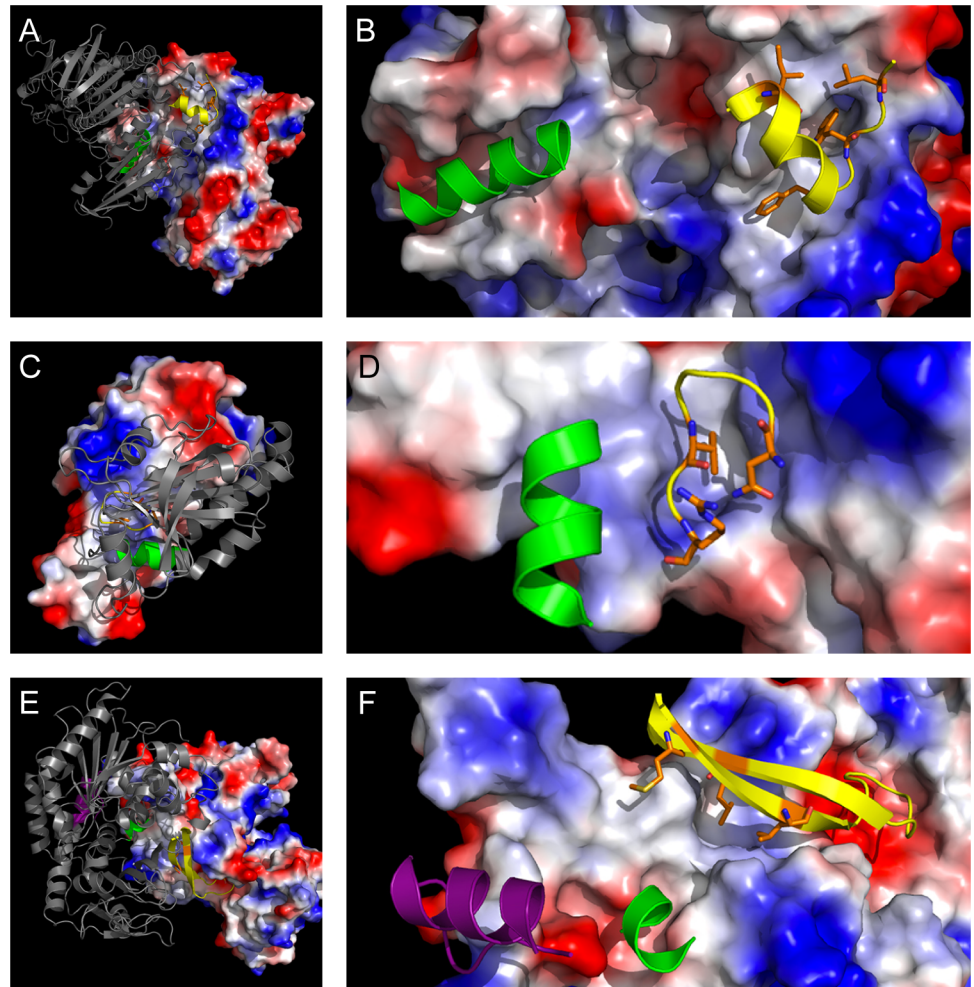


**Fig 1. Protein-protein interactions of drug targets involved in redox homeostasis.** (A) TryR dimer from *C. fasciculata* (PDB: 1FEC) with known inhibitory helix (green cartoon) and predicted inhibitory helix-terminating loop (yellow cartoon) against calculated electrostatic surface. (B) Detail of interface peptide 71-TIRESAGFGWELD containing hot spots Ile-72, Phe-78, Trp-80, and Leu-82 (orange sticks). (C) TXNPx dimer from *L. major* (PDB: 4K1F) with predicted helix from HippDB (green cartoon) and predicted inhibitory loop (yellow cartoon) against calculated electrostatic surface. (D) Detail of interface peptide 145-NDMPVGR containing hot spots Asn-145, Val-149, and Arg-151 (orange sticks). (E) G6PDH dimer from *T. cruzi* (PDB: 4E9I) with predicted helix from HippDB (green cartoon), helix-turn predicted by Loopfinder (purple cartoon), and long, beta-sheet-anchored loop (yellow cartoon) matching the homologous region of a known inhibitor of *H. sapiens* G6PDH. (F) Detail of interface peptide 441-AMYLKLTAKTPGLLDNDTHQTEL containing hot spots Met-442, Leu-446, and Leu-462 (orange sticks) clustered in a hydrophobic pocket. Images were rendered using PyMOL v0.99rc6 [42].

<https://doi.org/10.1371/journal.pntd.0005720.g001>

required for TS<sub>2</sub> reduction [37]. G6PDH is both an essential enzyme and a validated drug target [51], in addition to being catalytically active in both dimeric and tetrameric forms. Inhibition by peptide-based PPI disruption has been successfully applied to human G6PDH [35]. This study identifies a homologous loop from *T. cruzi*, 441-AMYLKLTAKTPGLLDNDTHQ-TEL, containing three hot spots, Met-442, Leu-446, and Leu-462, which are tightly clustered on adjacent strands of a beta sheet in a hydrophobic cleft (Fig 1). This suggests that this approach may find similar success in trypanosomatids with a carefully designed, smaller macrocyclic peptide. Moreover, Peptiderive identifies a decameric segment predicted to contribute

38% of interface energy, which, when extended to include an adjacent two-turn helix, is expected to contribute >50% of interface energy by Loopfinder (heat score: 4). Considering the successful inhibition of hG6PDH and a second predicted inhibitory peptide, G6PDH presents a logical opportunity to explore PPI-based inhibition.

6-phosphogluconate dehydrogenase catalyzes the third step in the pentose phosphate pathway, converting 6-phosphogluconate to ribulose 5-phosphate and CO<sub>2</sub>. G6PDH and 6PGDH are the primary source of NADPH for the reduction of TS<sub>2</sub> [37,52,53]. This essential enzyme has a highly conserved sequence identity between *T. cruzi*, *T. brucei*, and *L. major*, yet differs substantially from the human 6PGDH homolog, making it an ideal drug target [54]. Substrate analogs have shown potent inhibition of 6PGDH and trypanocidal activity in the low micromolar range [55]. Substrate binding involves residues from both protomers, suggesting PPI disruption may also be a viable inhibition strategy [56]. This study identifies a loop in *T. brucei* 6PGDH, 251-LTEHVMDRI, containing three hot spots, Asp-253, Val-255, and Ile-259. HippDB, Loopfinder, and Peptiderive all identified peptides immediately surrounding a helix, 445-YGQLVSLQRDVFG, predicted to contribute 10–13% of the interface energy.

### Essential enzymes beyond trypanothione metabolism

The remaining seven targets represent a variety of essential metabolic and biosynthetic processes. Two targets emerged in sugar metabolism: ribose-5-phosphate isomerase B (RpiB) in the non-oxidative branch of the PPP and UDP-glucose-4'-epimerase (GalE) in galactose catabolism. Three other targets are involved in varied essential biosynthetic processes: Farnesyl pyrophosphate synthase (FPPS) in the isoprenoid biosynthetic pathway, tyrosine aminotransferase (TAT) in tyrosine catabolism, and pteridine reductase (PTR1) in cofactor biosynthesis. Finally, two essential targets are found in nucleotide synthesis: deoxyuridine triphosphate nucleotidohydrolase (dUTPase) and dihydroorotate dehydrogenase (DHODH).

Ribose 5-phosphate isomerase B catalyzes the interconversion of D-ribose-5-phosphate and D-ribulose-5-phosphate in the non-oxidative branch of the pentose phosphate pathway. RpiB is essential for viability of the bloodstream form of *T. brucei* and is a subtype with no mammalian homologue [57–59]. RpiBs are functionally obligate dimers, with catalytic residues spanning both subunits, suggesting that targeting the RpiB interface may be a viable inhibition strategy. The peptide sequence from *T. cruzi* RpiB identified in this study overlaps a helix predicted by HippDB to contribute 49% of the interface energy. This helix, 140-RRIE-KIRAIEASH, contains two predicted hot spots, Ile-145 and Ile-148, on adjacent turns of the helix and the indispensable residue Glu-149. Experimental mutation of this residue disrupts both structure and function in *LdRpiB* [60]. This helix is also immediately C-terminal to His-138, another deactivating mutant (Fig 2). All four amino acid residues are conserved between *T. cruzi* and *L. donovani*, suggesting the generality of a peptide helix-based inhibitor.

UDP-galactose-4'-epimerase is an essential enzyme for the growth and survival of trypanosomatid parasites [61]. Unable to acquire galactose from the host, they rely on GalE to synthesize galactose from glucose [61,62]. *T. brucei* GalE has 33% homology to the human enzyme [63], and thus has received substantial attention as a target for trypanocidal drugs. Several small-molecule inhibitors have been identified, mainly targeting the active site of the enzyme [62,64,65]. Additionally, GalE is only fully functional as a dimer [61,62], suggesting that the interface of this enzyme is potentially druggable. This study identifies a helix, 111-PLKYDNNVVGILRLL, with two hotspots, Val-119 and Ile-123, on adjacent turns of the same buried helical face of *T. brucei* GalE, overlapping sequences identified by both HippDB (33% interface energy) and Loopfinder (heat score: 9) (Fig 2).

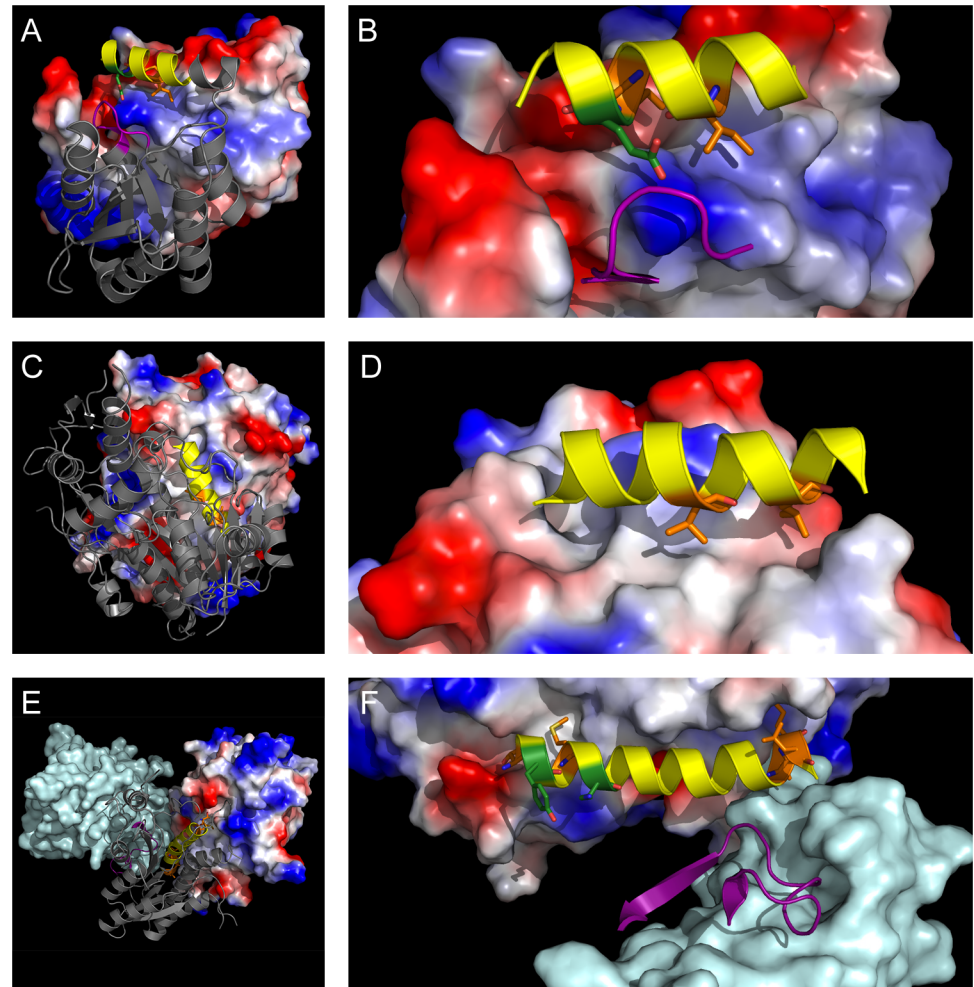


**Fig 2. Other essential enzymes where PPI disruption may be a viable inhibition strategy.** (A) RpiB dimer from *T. cruzi* (PDB: 3M1P) with predicted inhibitory loop (purple cartoon) and helix (yellow cartoon) against calculated electrostatic surface. (B) Detail of peptide 141-RIEKIRAIEASH containing hot spots Ile-145 and Ile-148 (orange sticks) and known inactivating mutant Glu-149 (green sticks). (C) GalE dimer from *T. brucei* (PDB: 1GY8) with inhibitory helix (yellow cartoon) predicted by HippDB, Loopfinder, Peptiderive, and this study against calculated electrostatic surface. (D) Detail of peptide 111-PLKYDNNVVGILRLL containing hot spots Val-119 and Leu-123 (orange sticks) on adjacent turns of the helix. (E) Chains A (grey cartoon), B (electrostatic surface), and C (pale blue surface) of PTR1 tetramer from *L. major* (PDB: 2QHJ) with predicted A-C interface inhibitory loop (purple cartoon) and A-B interface inhibitory helix (yellow cartoon). (F) Detail of PTR1 helix 5, 192-TIYTMAGALEGLTRSAALELA, containing predicted hotspots Thr-192, Met-196, Leu-210, Glu-211, and Leu-212 (orange sticks) and catalytic residues Tyr-194 and Lys-198 (green sticks). Images were rendered using PyMOL v0.99rc6 [42].

<https://doi.org/10.1371/journal.pntd.0005720.g002>

Farnesyl diphosphate synthase, a key enzyme in sterol biosynthesis, catalyzes the sequential condensation of isopentenyl diphosphate and dimethylallyl diphosphate to form geranyl diphosphate and ultimately farnesyl diphosphate, which is the obliged precursor for the biosynthesis of sterols, ubiquinones, dolichols, heme A, and prenylated proteins [66]. Recently, FPPS has been validated as a drug target [67] and the sterol biosynthesis pathway has been targeted at numerous other steps [68]. Most established inhibitors are bisphosphonate substrate mimics; however, they are commonly associated with poor drug-like characteristics [69–72]. FPPS is a functionally obligate homodimer, with the active site located at the protein-protein



interface [66,73]. This study identifies a turn between two helices, 25-FDMDPNRVRYL containing three hotspots, Phe-25, Tyr-34, and Leu-35, in *T. brucei* FPPS [66]. This same segment is identified by both Peptiderive (15% interface energy) and Loopfinder (heat score: 3).

Tyrosine aminotransferase, which is involved in the first step of amino acid catabolism, catalyzes transamination for both dicarboxylic and aromatic amino-acid substrates [74]. Structural studies suggest that TAT is only fully functional in the dimeric state [75]. TAT is overexpressed in *T. cruzi* from patients with acute Chagas [76] and associated with resistance to oxidative damage. This study identifies a three-turn interface helix, 54-AQIKKLKEAIDS, in *T. cruzi* and *L. infantum* TAT with two proximal hotspots, Leu-59 and Ile-63, on adjacent turns, presenting a hydrophobic face buried in the opposite protomer. This is in contrast to the only helix found in HippDB, 275-PSFLEGLKRVGMLV (15% interface energy), which interacts primarily with the domain-swapped, N-terminal 15 amino acids.

Pteridine reductase, a short-chain reductase, participates in the salvage of pterins, for which trypanosomatids are auxotrophic [77]. PTR1 catalyzes the NADPH-dependent two-stage reduction of oxidized pterins to the active tetrahydro-forms and provides an alternate pathway for folate reduction, allowing *de novo* thymidylate synthesis to occur even in the presence of methotrexate [77,78]. PTR1 is essential in *T. brucei* and has been targeted in numerous small-molecule efforts [79–82]. The enzyme is a functional tetramer with substantial surface contacts between the A chain and B and C chains [79,83], suggesting the viability of targeting the PPI. This study identifies six hotspots on helix 5 of *L. major* PTR1, with hotspots clustered in hydrophobic pockets at the N-terminal (Thr-192 and Met-196) and C-terminal (Leu-210, Glu-211, Leu-212, and Leu-215) ends of an otherwise convex surface at the A-B interface (Fig 2). The C-terminal portion of this helix is predicted by Peptiderive to contribute 24% of the A-B interface energy and is positioned to mediate the A-C interaction as well. This same helix was identified by HippDB (67% A-B interface energy) and contains two key catalytic residues, Tyr-194 and Lys-198, mutation of which inactivates PTR1 [84]. Loopfinder identified a complementary loop (heat score: 9) that appears to contribute substantially to the A-C interaction.

Deoxyuridine triphosphate nucleotidohydrolase is necessary for both DNA repair and *de novo* synthesis of dTTP. It converts dTUP to dUMP and pyrophosphate. dUTPase maintains a high ratio of dTTP:dUTP, preventing accidental incorporation of uracil into DNA [85,86]. This enzyme was shown to be essential in *L. major* and *T. brucei* with decreased proliferation in both the procyclic and bloodstream forms of the organism [85,87]. *T. cruzi* dUTPase, an obligate dimer, shows little homology to the human counterpart, which is a functional monomer, contributing to its potential as a drug target [86,87]. However, among trypanosomatids, the interface residues are highly conserved [85]. This study identifies an unstructured loop on the interface of *L. major* dUTPase, 51-ELLDSYPWKWWK, with two hotspots, Leu-53, Trp-58, in close proximity. An overlapping segment was identified by Peptiderive (35% interface energy). Trp-58, Trp-60, and Trp-61 are buried in a deep hydrophobic cavity on the opposite protomer, although only the former was identified by this computational alanine scan.

Dihydroorotate dehydrogenase catalyzes the oxidation of dihydroorotate to orotate in the *de novo* pyrimidine biosynthetic pathway [88]. The highly conserved DHODHs found in trypanosomatids bear less than 20% sequence homology to the analogous human enzyme [89,90]. DHODH knockout studies demonstrated that the protein is essential in *T. cruzi* and an obligate dimer [89,90], suggesting that DHODH would be an ideal drug target in trypanosomatids. This study identifies a long, unstructured loop in *T. brucei* DHODH, 202-VIDAE-TESVVIKPKQGFG, containing three hotspots, Ile-203, Val-210, and Phe-218, tightly clustered in a hydrophobic groove. Both Loopfinder (heat score: 3) and Peptiderive (23% interface energy) identify overlapping portions of this peptide, suggesting an ideal starting point for the development of macrocyclic inhibitors.



**Table 2. Classes of multi-chain kinetoplastid enzymes with structural data in the PDB.**

Enzyme Class	Number	Percent
Oxidoreductases	38	18.4%
Transferases	44	21.3%
Hydrolases	23	11.1%
Lyases	18	8.7%
Isomerases	18	8.7%
Ligases	7	3.4%
<b>Total</b>	<b>148</b>	<b>71.5%</b>

<https://doi.org/10.1371/journal.pntd.0005720.t002>

## General trends and future outlook

In the past decade, inhibition of PPIs has evolved from the short, primary epitopes exemplified by RGD-peptide-like integrin antagonists and AVPI-peptide-like Smac mimetics to include clinically relevant molecules that recapitulate increasingly complex secondary and tertiary structures like those presented by the BCL family and IL-2, respectively [12,91]. The diversity of topologies, interaction motifs, and binding affinities at these interfaces presents an intriguing challenge for the development of new PPI inhibitors [7]. PPI-based inhibition of NTD targets has achieved some pre-clinical successes, including non-peptide inhibitors of the cysteine protease cruzain [92,93], and interface-peptide-derived inhibitors of triosephosphate isomerase [14,16].

Ultimately, this analysis identified solely homomultimeric enzymes. This is likely due to the bias of existing structural data towards these types of targets, which have received substantial attention as targets for structure-based design of small-molecule inhibitors [28,31,94]. Of the 207 multi-chain trypanosomatid crystal structures in the PDB, 148 (71.5%) are for enzymes (Table 2). Nevertheless, two of the 12 targets identified in this study have been successfully inhibited by interface-derived peptides. An interface-derived peptide helix has been demonstrated to inhibit *Li*TryR through a mechanism that disrupts the PPI [34,40]. This helix had also been identified by HippDB as potentially contributing 15% of the interface energy, while the loop region identified in this analysis is predicted to contribute 22%. Similarly, the G6PDH interface peptide matches a homologous region in the human enzyme, which has been successfully developed into an inhibitory peptide [35]. Given the proximity of the hot spots in space rather than sequence, it appears amenable to inhibition by a macrocycle or peptidomimetic. Overall, PPI-based inhibition of multimeric enzymes [14,15] represents a complementary, but underutilized, approach to these targets.

The interface peptides identified in this study predominantly contain hot-spot amino acids with aliphatic side chains (Leu, 29%; Ile, 24%; Val, 12%) and Phe (9%). Surprisingly [95–97], other aromatic amino acids (Tyr, 3%; Trp, 3%) appear to be underrepresented in this analysis. These percentages do not differ substantially from the hot spots found over the entire interface (Leu, 30%; Ile, 16%; Val, 16%; Phe, 13%; Tyr, 3%; Trp, 2%). Bogan and Thorn observed a general enrichment of Trp, Tyr, and Arg at interface hot spots [98]; the Loopfinder dataset observed enrichment of Trp, Phe, His, Asp, Tyr, Leu, Glu, and Ile in hot loops [25]. This contrast is most apparent when examining specific PPIs in this study. In the case of TryR (Fig 1), an experimentally verified hot spot (Trp-80) [34] was not identified by the computational alanine scan, despite being buried in the opposite chain of the protein. TryR Trp-80 is conserved across kinetoplastids (S5 Table), as are two of the three calculated hot spots, Ile/Leu-71 and Phe-78. Similarly, the hydrophobic face presented by the interface helix identified for GalE contains a third residue, Tyr-115, not identified in this analysis, but contained in the single

alpha-turn found by HippDB as contributing 33% of interface energy (Fig 2). As in the case of TryR, the GalE interface peptide contains three highly conserved hotspots, Pro-111, Val-119, Leu/Ile-123. Sequence conservation of both interface peptides and hot spots was highly variable from protein to protein, with large differences in enzymes such as G6PDH and RpiB, but high homology in TXNPx and PTR1 (S5 Table). Overall, since the interface peptides were identified manually rather than algorithmically, and this is a relatively small data set, it is impractical to extrapolate broader conclusions about the nature of potentially inhibitory interface peptides.

## Conclusion

Computational alanine scanning has revealed 12 drug targets in kinetoplastid parasites that are likely amenable to PPI-based inhibition. While all 12 targets are covered by previous PDB-wide analyses focusing on particular structural motifs, manual inspection of this subset has revealed a number of unique sequences that provide a logical starting point for the development of new inhibitors. Nine of the identified targets have sequences overlapping those identified in previous databases, and two have been experimentally verified, suggesting the potential generality of PPI-based inhibition for these homomultimeric enzymes. Moreover, this approach leverages the power of freely available databases and computational tools, allowing for the rapid analysis of newly disclosed structures for novel modes of inhibition. While a generally predictive model of PPI inhibition has yet to be established, the targets identified in this work present particularly attractive opportunities for the exploration of new modes of inhibition for these targets.

## Supporting information

**S1 Fig. Sequence and structural alignment of *Li*TryR and hGR inhibitory peptides.** Structure alignment of the inhibitory peptide helices for *Li*TryR (435-PEIIQSVGICMKM, shown in purple) and hGR (436-QQLGCDEMLQGFVAVKMGATKAD, shown in teal) taken from PDB structures 2JK6 and 1GRE. In the assumed binding conformation, *Li*TryR residues E436, Q439, I443, K446, and M447 (purple sticks) present a nearly identical buried helical face to hGR residues E442, Q445, V449, K452, and M453 (teal sticks). Image was rendered using PyMOL v0.99rc6 [42].

(TIF)

**S1 Table. Full comparison of predicted peptide inhibitor sequences with existing databases and tools.** HippDB and Peptiderive scores are both listed as % interface energy contributed by the peptide. Loopfinder heat score is determined using three criteria: A) average amino acid  $\geq 0.6$  REU; B)  $\geq 3$  hot spots; C) contributes  $> 50\%$  interface energy. A heat score of 2, 3, or 4 meets only condition A, B, or C, respectively; a heat score of 9 meets all three criteria.

(XLSX)

**S2 Table. List of interface hot spots identified for PPIs highlighted in Table 1.**

(XLSX)

**S3 Table. All PPIs containing at least three interface hot spots.**

(XLSX)

**S4 Table. All multimeric protein interfaces considered in this study.**

(XLS)

**S5 Table. Comparison of interface peptide sequences across kinetoplastid species.**

(XLSX)

## Author Contributions

**Conceptualization:** Jason Gavenonis.

**Investigation:** Leah M. Wachsmuth, Meredith G. Johnson, Jason Gavenonis.

**Methodology:** Leah M. Wachsmuth, Jason Gavenonis.

**Software:** Jason Gavenonis.

**Supervision:** Jason Gavenonis.

**Visualization:** Leah M. Wachsmuth, Meredith G. Johnson, Jason Gavenonis.

**Writing – original draft:** Leah M. Wachsmuth, Meredith G. Johnson, Jason Gavenonis.

**Writing – review & editing:** Leah M. Wachsmuth, Meredith G. Johnson, Jason Gavenonis.

## References

1. Global, regional, and national age–sex specific all-cause and cause-specific mortality for 240 causes of death, 1990–2013: a systematic analysis for the Global Burden of Disease Study 2013. *Lancet*. 2015; 385: 117–171. [https://doi.org/10.1016/S0140-6736\(14\)61682-2](https://doi.org/10.1016/S0140-6736(14)61682-2) PMID: 25530442
2. Pink R, Hudson A, Mouriès M-A, Bendig M. Opportunities and challenges in antiparasitic drug discovery. *Nat Rev Drug Discov*. 2005; 4: 727–740. <https://doi.org/10.1038/nrd1824> PMID: 16138106
3. Peacock CS, Seeger K, Harris D, Murphy L, Ruiz JC, Quail MA, et al. Comparative genomic analysis of three *Leishmania* species that cause diverse human disease. *Nat Genet*. 2007; 39: 839–847. <https://doi.org/10.1038/ng2053> PMID: 17572675
4. Patel G, Roncal NE, Lee PJ, Leed SE, Erath J, Rodriguez A, et al. Repurposing human Aurora kinase inhibitors as leads for anti-protozoan drug discovery. *Medchemcomm*. 2014; 5: 655. <https://doi.org/10.1039/C4MD00045E> PMID: 24910766
5. Pizarro JC, Hills T, Senisterra G, Wernimont AK, Mackenzie C, Norcross NR, et al. Exploring the *Trypanosoma brucei* Hsp83 Potential as a Target for Structure Guided Drug Design. *PLoS Negl Trop Dis*. 2013; 7: e2492. <https://doi.org/10.1371/journal.pntd.0002492> PMID: 24147171
6. Wells JA, McClendon CL. Reaching for high-hanging fruit in drug discovery at protein-protein interfaces. *Nature*. 2007; 450: 1001–9. <https://doi.org/10.1038/nature06526> PMID: 18075579
7. Smith MC, Gestwicki JE. Features of protein–protein interactions that translate into potent inhibitors: topology, surface area and affinity. *Expert Rev Mol Med*. 2012; 14: e16. <https://doi.org/10.1017/erm.2012.10> PMID: 22831787
8. Clackson T, Wells JA. A hot spot of binding energy in a hormone-receptor interface. *Science*. 1995; 267: 383–6. <https://doi.org/10.1126/science.7529940> PMID: 7529940
9. Kortemme T, Baker D. A simple physical model for binding energy hot spots in protein-protein complexes. *Proc Natl Acad Sci U S A*. 2002; 99: 14116–14121. <https://doi.org/10.1073/pnas.202485799> PMID: 12381794
10. Bourgeas R, Basse M-J, Morelli X, Roche P. Atomic Analysis of Protein-Protein Interfaces with Known Inhibitors: The 2P2I Database. Fernandez-Fuentes N, editor. *PLoS One*. 2010; 5: e9598. <https://doi.org/10.1371/journal.pone.0009598> PMID: 20231898
11. Marsault E, Peterson ML. Macrocycles Are Great Cycles: Applications, Opportunities, and Challenges of Synthetic Macrocycles in Drug Discovery. *J. Med. Chem*. 2011; 54:1961–2004. <https://doi.org/10.1021/jm1012374> PMID: 21381769
12. Arkin MR, Tang Y, Wells JA. Small-molecule inhibitors of protein-protein interactions: Progressing toward the reality. *Chem Biol*. 2014; 21: 1102–1114. <https://doi.org/10.1016/j.chembiol.2014.09.001> PMID: 25237857
13. Sajid M, Robertson SA, Brinen LS, McKerrow JH. Cruzain. In: Mark W. Robinson, Dalton John P., editors. *Cysteine Proteases of Pathogenic Organisms*. 2011. pp. 100–115. [https://doi.org/10.1007/978-1-4419-8414-2\\_7](https://doi.org/10.1007/978-1-4419-8414-2_7) PMID: 21660661
14. Singh SK, Maithal K, Balaram H, Balaram P. Synthetic peptides as inactivators of multimeric enzymes: Inhibition of *Plasmodium falciparum* triosephosphate isomerase by interface peptides. *FEBS Lett*. 2001; 501: 19–23. [https://doi.org/10.1016/S0014-5793\(01\)02606-0](https://doi.org/10.1016/S0014-5793(01)02606-0) PMID: 11457449

15. Cardinale D, Salo-Ahen OMH, Ferrari S, Ponterini G, Cruciani G, Carosati E, et al. Homodimeric enzymes as drug targets. *Curr Med Chem*. 2010; 17: 826–846. <https://doi.org/10.2174/092986710790712156> PMID: 20156173
16. Olivares-Illana V, Rodríguez-Romero A, Becker I, Berzunza M, García J, Pérez-Montfort R, et al. Perturbation of the dimer interface of triosephosphate isomerase and its effect on *Trypanosoma cruzi*. *PLoS Negl Trop Dis*. 2007; 1: e1. <https://doi.org/10.1371/journal.pntd.0000001> PMID: 17989778
17. RCSB Protein Data Bank—RCSB PDB [Internet]. [cited 22 Apr 2016]. Available: <http://www.rcsb.org/pdb/home/home.do>
18. Chaudhury S, Lyskov S, Gray JJ. PyRosetta: A script-based interface for implementing molecular modeling algorithms using Rosetta. *Bioinformatics*. 2010; 26: 689–691. <https://doi.org/10.1093/bioinformatics/btq007> PMID: 20061306
19. Index of /pyrosetta/downloads/pyrosetta\_scripts [Internet]. [cited 22 May 2017]. Available: [http://graylab.jhu.edu/pyrosetta/downloads/pyrosetta\\_scripts/](http://graylab.jhu.edu/pyrosetta/downloads/pyrosetta_scripts/)
20. O'Meara MJ, Leaver-Fay A, Tyka MD, Stein A, Houlihan K, Dimaio F, et al. Combined covalent-electrostatic model of hydrogen bonding improves structure prediction with Rosetta. *J Chem Theory Comput*. 2015; 11: 609–622. <https://doi.org/10.1021/ct500864r> PMID: 25866491
21. Shulman-Peleg A, Shatsky M, Nussinov R, Wolfson HJ. Spatial chemical conservation of hot spot interactions in protein-protein complexes. *BMC Biol*. 2007; 5: 43. <https://doi.org/10.1186/1741-7007-5-43> PMID: 17925020
22. London N, Raveh B, Movshovitz-Attias D, Schueler-Furman O. Can self-inhibitory peptides be derived from the interfaces of globular protein-protein interactions? *Proteins Struct Funct Bioinforma*. 2010; 78: 3140–3149. <https://doi.org/10.1002/prot.22785> PMID: 20607702
23. Bergey CM, Watkins AM, Arora PS. HippDB: A database of readily targeted helical protein-protein interactions. *Bioinformatics*. 2013; 29: 2806–2807. <https://doi.org/10.1093/bioinformatics/btt483> PMID: 23958730
24. Bullock BN, Jochim AL, Arora PS. Assessing Helical Protein Interfaces for Inhibitor Design. *J Am Chem Soc*. 2011; 133: 14220–14223. <https://doi.org/10.1021/ja206074j> PMID: 21846146
25. Gavenonis J, Sheneman BA, Siegert TR, Eshelman MR, Kritzer JA. Comprehensive analysis of loops at protein-protein interfaces for macrocycle design. *Nat Chem Biol*. 2014; 10: 716–22. <https://doi.org/10.1038/nchembio.1580> PMID: 25038791
26. Siegert TR, Bird M, Kritzer JA. Identifying Loop-Mediated Protein–Protein Interactions Using LoopFinder. *Methods in Molecular Biology* 2017: 1561 pp. 255–277. [https://doi.org/10.1007/978-1-4939-6798-8\\_15](https://doi.org/10.1007/978-1-4939-6798-8_15) PMID: 28236243
27. Duschak VG. A decade of targets and patented drugs for chemotherapy of chagas disease. *Recent Pat Antiinfect Drug Discov*. 2011; 6: 216–259. <https://doi.org/10.2174/157489111796887864> PMID: 21824073
28. Comini MA, Ortíz C, Cazzulo JJ. Drug Targets in Trypanosomal and Leishmanial Pentose Phosphate Pathway. *Trypanosomatid Diseases: Molecular Routes to Drug Discovery*. 2013; 297–313. <https://doi.org/10.1002/9783527670383.ch16>
29. Rodenko B, De Koning HP. Rational Selection of Anti-Microbial Drug Targets: Unique or Conserved? *Trypanosomatid Diseases: Molecular Routes to Drug Discovery*. 2013; 279–296. <https://doi.org/10.1002/9783527670383.ch15>
30. Krauth-Siegel RL, Bauer H, Schirmer RH. Dithiol proteins as guardians of the intracellular redox milieu in parasites: Old and new drug targets in trypanosomes and malaria-causing plasmodia. *Angew Chemie—Int Ed*. 2005; 44: 690–715. <https://doi.org/10.1002/anie.200300639> PMID: 15657967
31. Flohé L. The trypanothione system and its implications in the therapy of trypanosomatid diseases. *Int J Med Microbiol*. 2012; 302: 216–220. <https://doi.org/10.1016/j.ijmm.2012.07.008> PMID: 22889611
32. Sedan Y, Marcu O, Lyskov S, Schueler-Furman O. Peptiderver: derive peptide inhibitors from protein–protein interactions. *Nucleic Acids Res*. 2016; 44: W536–W541. <https://doi.org/10.1093/nar/gkw385> PMID: 27141963
33. Units in Rosetta [Internet]. [cited 25 May 2017]. Available: [https://www.rosettacommons.org/docs/latest/rosetta\\_basics/Units-in-Rosetta](https://www.rosettacommons.org/docs/latest/rosetta_basics/Units-in-Rosetta)
34. Toro MA, Sanchez-Murcia PA, Moreno D, Ruiz-Santaquiteria M, Alzate JF, Negri A, et al. Probing the Dimerization Interface of *Leishmania infantum* Trypanothione Reductase with Site-Directed Mutagenesis and Short Peptides. *ChemBioChem*. 2013; 14: 1212–1217. <https://doi.org/10.1002/cbic.201200744> PMID: 23744811
35. Obiol-Pardo C, Alcarraz-Vizán G, Díaz-Moralli S, Cascante M, Rubio-Martinez J, Alcarraz-Vizán G, et al. Design of an interface peptide as new inhibitor of human glucose-6-phosphate dehydrogenase. *J Mol Graph Model*. 2014; 49: 110–117. <https://doi.org/10.1016/j.jmgl.2014.02.004> PMID: 24637073



36. Comini MA, Flohé L. Trypanothione-Based Redox Metabolism of Trypanosomatids. *Trypanosomatid Diseases: Molecular Routes to Drug Discovery*. 2013. 167–199. <https://doi.org/10.1002/9783527670383.ch9>
37. Igoillo-Esteve M, Maugeri D, Stern AL, Beluardi P, Cazzulo JJ. The pentose phosphate pathway in *Trypanosoma cruzi*: a potential target for the chemotherapy of Chagas disease. *An Acad Bras Cienc*. 2007; 79: 649–663. S0001-37652007000400007 [pii] PMID: 18066434
38. Bernardes LSC, Zani CL, Carvalho I. Trypanosomatidae diseases: from the current therapy to the efficacious role of trypanothione reductase in drug discovery. *Curr Med Chem*. 2013; 20: 2673–96. <https://doi.org/10.2174/0929867311320210005> PMID: 23410156
39. Holloway GA, Charman WN, Fairlamb AH, Brun R, Kaiser M, Kostewicz E, et al. Trypanothione reductase high-throughput screening campaign identifies novel classes of inhibitors with antiparasitic activity. *Antimicrob Agents Chemother*. 2009; 53: 2824–2833. <https://doi.org/10.1128/AAC.01568-08> PMID: 19364854
40. Sánchez-Murcia P, Ruiz-Santaquiteria M, Toro M, de Lucio H, Jiménez MÁ, Gago F, et al. Comparison of hydrocarbon-and lactam-bridged cyclic peptides as dimerization inhibitors of *Leishmania infantum* trypanothione reductase. *RSC Adv*. 2015; 5: 55784–55794. <https://doi.org/10.1039/C5RA06853C>
41. Nordhoff a, Tziatzios C, van den Broek J a, Schott MK, Kalbitzer HR, Becker K, et al. Denaturation and reactivation of dimeric human glutathione reductase—an assay for folding inhibitors. *Eur J Biochem*. 1997; 245: 273–282. <https://doi.org/10.1111/j.1432-1033.1997.00273.x> PMID: 9151953
42. DeLano WL. *The PyMOL Molecular Graphics System*. Palo Alto, CA, USA: DeLano Scientific; 2002.
43. Pratt C, Nguyen S, Phillips MA. Genetic Validation of *Trypanosoma brucei* Glutathione Synthetase as an Essential Enzyme. *Eukaryot Cell*. 2014; 13: 614–624. <https://doi.org/10.1128/EC.00015-14> PMID: 24610661
44. Fyfe PK, Alphey MS, Hunter WN. Structure of *Trypanosoma brucei* glutathione synthetase: Domain and loop alterations in the catalytic cycle of a highly conserved enzyme. *Mol Biochem Parasitol*. 2010; 170: 93–99. <https://doi.org/10.1016/j.molbiopara.2009.12.011> PMID: 20045436
45. Pratt CB. *The Role of Glutathione Synthetase in Trypanothione Biosynthesis in Trypanosoma brucei*. Ph.D. Thesis, The University of Texas Southwestern Medical Center. 2013.
46. Fueller F, Jehle B, Putzkers K, Lewiss JD, Krauth-Siegel RL. High throughput screening against the peroxidase cascade of African trypanosomes identifies antiparasitic compounds that inactivate trypanoperoxidase. *J Biol Chem*. 2012; 287: 8792–8802. <https://doi.org/10.1074/jbc.M111.338285> PMID: 22275351
47. Diechtierow M, Krauth-Siegel RL. A trypanoperoxidase-dependent peroxidase protects African trypanosomes from membrane damage. *Free Radic Biol Med*. 2011; 51: 856–868. <https://doi.org/10.1016/j.freeradbiomed.2011.05.014> PMID: 21640819
48. Brindisi M, Brogi S, Relitti N, Vallone A, Butini S, Gemma S, et al. Structure-based discovery of the first non-covalent inhibitors of *Leishmania major* trypanoperoxidase by high throughput docking. *Sci Rep*. 2015; 5: 9705. <https://doi.org/10.1038/srep09705> PMID: 25951439
49. Mutlu O. In silico molecular modeling and docking studies on the leishmanial trypanoperoxidase. *Brazilian Arch Biol Technol*. 2014; 57: 244–252. <https://doi.org/10.1590/S1516-89132014000200013>
50. Lu J, Vodnala SK, Gustavsson A-L, Gustafsson TN, Sjöberg B, Johansson HA, et al. Ebsulfur is a benzothiazolone cytotoxic inhibitor targeting the trypanothione reductase of *Trypanosoma brucei*. *J Biol Chem*. 2013; 288: 27456–68. <https://doi.org/10.1074/jbc.M113.495101> PMID: 23900839
51. Cordeiro AT, Thiemann OH. 16-Bromoepiandrosterone, an activator of the mammalian immune system, inhibits glucose 6-phosphate dehydrogenase from *Trypanosoma cruzi* and is toxic to these parasites grown in culture. *Bioorganic Med Chem*. 2010; 18: 4762–4768. <https://doi.org/10.1016/j.bmc.2010.05.008> PMID: 20570159
52. Montin K. Characterization of the mechanism of 6-phosphogluconate dehydrogenase from *trypanosoma brucei* and its interaction with inhibitors by isothermal titration calorimetry. Ph.D. Thesis; Università di Ferrara; 2009.
53. Hanau S, Rippa M, Bertelli M, Dalocchio F, Barrett MP. 6-Phosphogluconate dehydrogenase from *Trypanosoma brucei*. Kinetic analysis and inhibition by trypanocidal drugs. *Eur J Biochem*. 1996; 240: 592–9. PMID: 8856059
54. Esteve MI, Cazzulo JJ. The 6-phosphogluconate dehydrogenase from *Trypanosoma cruzi*: The absence of two inter-subunit salt bridges as a reason for enzyme instability. *Mol Biochem Parasitol*. 2004; 133: 197–207. <https://doi.org/10.1016/j.molbiopara.2003.10.007> PMID: 14698432
55. Ruda GF, Alibu VP, Mitsos C, Bidet O, Kaiser M, Brun R, et al. Synthesis and biological evaluation of phosphate prodrugs of 4-phospho-D-erythronohydroxamic acid, an inhibitor of 6-phosphogluconate dehydrogenase. *ChemMedChem*. 2007; 2: 1169–1180. <https://doi.org/10.1002/cmdc.200700040> PMID: 17615587

56. Montin K, Cervellati C, Dallochio F, Hanau S. Thermodynamic characterization of substrate and inhibitor binding to *Trypanosoma brucei* 6-phosphogluconate dehydrogenase. *FEBS J.* 2007; 274: 6426–35. <https://doi.org/10.1111/j.1742-4658.2007.06160.x> PMID: 18021252
57. Faria J, Loureiro I, Santarém N, Cecílio P, Macedo-Ribeiro S, Tavares J, et al. Disclosing the essentiality of ribose-5-phosphate isomerase B in *Trypanosomatids*. *Sci Rep.* 2016; 6: 26937. <https://doi.org/10.1038/srep26937> PMID: 27230471
58. Loureiro I, Faria J, Clayton C, Macedo-Ribeiro S, Santarém N, Roy N, et al. Ribose 5-Phosphate Isomerase B Knockdown Compromises *Trypanosoma brucei* Bloodstream Form Infectivity. *PLoS Negl Trop Dis.* 2015; 9: 1–11. <https://doi.org/10.1371/journal.pntd.0003430> PMID: 25568941
59. Stern AL, Burgos E, Salmon L, Cazzulo JJ. Ribose 5-phosphate isomerase type B from *Trypanosoma cruzi*: kinetic properties and site-directed mutagenesis reveal information about the reaction mechanism. *Biochem J.* 2007; 401: 279–285. <https://doi.org/10.1042/BJ20061049> PMID: 16981853
60. Kaur PK, Tripathi N, Desale J, Neelagiri S, Yadav S, Bharatam P V., et al. Mutational and Structural Analysis of Conserved Residues in Ribose-5-Phosphate Isomerase B from *Leishmania donovani*: Role in Substrate Recognition and Conformational Stability. Salsbury F, editor. *PLoS One.* 2016; 11: e0150764. <https://doi.org/10.1371/journal.pone.0150764> PMID: 26953696
61. Alphey MS, Burton A, Urbaniak MD, Boons G-J, Ferguson MAJ, Hunter WN. *Trypanosoma brucei* UDP-galactose-4'-epimerase in ternary complex with NAD<sup>+</sup> and the substrate analogue UDP-4-deoxy-4-fluoro- $\alpha$ -D-galactose. *Acta Crystallogr Sect F Struct Biol Cryst Commun.* 2006; 62: 829–834. <https://doi.org/10.1107/S1744309106028740> PMID: 16946458
62. Friedman AJ, Durrant JD, Pierce LCT, McCorvie TJ, Timson DJ, McCammon JA. The Molecular Dynamics of *Trypanosoma brucei* UDP-Galactose 4'-Epimerase: A Drug Target for African Sleeping Sickness. *Chem Biol Drug Des.* 2012; 80: 173–181. <https://doi.org/10.1111/j.1747-0285.2012.01392.x> PMID: 22487100
63. Shaw MP, Bond CS, Roper JR, Gourley DG, Ferguson MAJ, Hunter WN. High-resolution crystal structure of *Trypanosoma brucei* UDP-galactose 4'-epimerase: a potential target for structure-based development of novel trypanocides. *Mol Biochem Parasitol.* 2003; 126: 173–180. [https://doi.org/10.1016/S0166-6851\(02\)00243-8](https://doi.org/10.1016/S0166-6851(02)00243-8) PMID: 12615316
64. Durrant JD, Urbaniak MD, Ferguson MAJ, McCammon JA. Computer-Aided Identification of *Trypanosoma brucei* Uridine Diphosphate Galactose 4'-Epimerase Inhibitors: Toward the Development of Novel Therapies for African Sleeping Sickness. *J Med Chem.* 2010; 53: 5025–5032. <https://doi.org/10.1021/jm100456a> PMID: 20527952
65. Urbaniak MD, Tabudravu JN, Msaki A, Matera KM, Brenk R, Jaspars M, et al. Identification of novel inhibitors of UDP-Glc 4'-epimerase, a validated drug target for african sleeping sickness. *Bioorg Med Chem Lett.* 2006; 16: 5744–5747. <https://doi.org/10.1016/j.bmcl.2006.08.091> PMID: 16962325
66. Gabelli SB, McLellan JS, Montalvetti A, Oldfield E, Docampo R, Amzel LM. Structure and mechanism of the farnesyl diphosphate synthase from *Trypanosoma cruzi*: Implications for drug design. *Proteins Struct Funct Bioinforma.* 2005; 62: 80–88. <https://doi.org/10.1002/prot.20754> PMID: 16288456
67. Dhar MK, Koul A, Kaul S. Farnesyl pyrophosphate synthase: a key enzyme in isoprenoid biosynthetic pathway and potential molecular target for drug development. *N Biotechnol.* 2013; 30: 114–123. <https://doi.org/10.1016/j.nbt.2012.07.001> PMID: 22842101
68. de Souza W, Rodrigues JCF. Sterol Biosynthesis Pathway as Target for Anti-trypanosomatid Drugs. *Interdiscip Perspect Infect Dis.* 2009; 2009: 642502. <https://doi.org/10.1155/2009/642502> PMID: 19680554
69. Rodriguez JB, Falcone BN, Szajnman SH. Approaches for Designing new Potent Inhibitors of Farnesyl Pyrophosphate Synthase. *Expert Opin Drug Discov.* 2016; 11: 307–320. <https://doi.org/10.1517/17460441.2016.1143814> PMID: 26781029
70. Liu Y-L, Cao R, Wang Y, Oldfield E. Farnesyl Diphosphate Synthase Inhibitors With Unique Ligand-Binding Geometries. *ACS Med Chem Lett.* 2015; 6: 349–354. <https://doi.org/10.1021/ml500528x> PMID: 25815158
71. Yang G, Zhu W, Kim K, Byun SY, Choi G, Wang K, et al. *In Vitro* and *In Vivo* Investigation of the Inhibition of *Trypanosoma brucei* Cell Growth by Lipophilic Bisphosphonates. *Antimicrob Agents Chemother.* 2015; 59: 7530–7539. <https://doi.org/10.1128/AAC.01873-15> PMID: 26392508
72. Demoro B, Caruso F, Rossi M, Benítez D, González M, Cerecetto H, et al. Bisphosphonate metal complexes as selective inhibitors of *Trypanosoma cruzi* farnesyl diphosphate synthase. *Dalt Trans.* 2012; 41: 6468. <https://doi.org/10.1039/c2dt12179d> PMID: 22344249
73. Szkopińska A, Plochocka D. Farnesyl diphosphate synthase; regulation of product specificity. *Acta Biochimica Polonica.* 2005; 52: 45–55. PMID: 15827605
74. Sobrado VR, Montemartini-Kalisz M, Kalisz HM, de la Fuente MC, Hecht H-J, Nowicki C. Involvement of conserved asparagine and arginine residues from the N-terminal region in the catalytic mechanism of

- rat liver and *Trypanosoma cruzi* tyrosine aminotransferases. *Protein Sci.* 2003; 12: 1039–1050. <https://doi.org/10.1110/ps.0229403> PMID: 12717026
75. Moreno MA, Abramov A, Abendroth J, Alonso A, Zhang S, Alcolea PJ, et al. Structure of tyrosine aminotransferase from *Leishmania infantum*. *Acta Crystallogr Sect F Struct Biol Commun.* 2014; 70: 583–587. <https://doi.org/10.1107/S2053230X14007845> PMID: 24817714
  76. Díaz ML, Solari A, González CI. Differential expression of *Trypanosoma cruzi* I associated with clinical forms of Chagas disease: Overexpression of oxidative stress proteins in acute patient isolate. *J Proteomics.* 2011; 74: 1673–1682. <https://doi.org/10.1016/j.jprot.2011.05.001> PMID: 21642025
  77. Nare B, Hardy LW, Beverley SM. The roles of pteridine reductase 1 and dihydrofolate reductase-thymidylate synthase in pteridine metabolism in the protozoan parasite *Leishmania major*. *J Biol Chem.* 1997; 272: 13883–91. <https://doi.org/10.1074/JBC.272.21.13883> PMID: 9153248
  78. Schüttelkopf AW, Hardy LW, Beverley SM, Hunter WN. Structures of *Leishmania major* Pteridine Reductase Complexes Reveal the Active Site Features Important for Ligand Binding and to Guide Inhibitor Design. *J Mol Biol.* 2005; 352: 105–116. <https://doi.org/10.1016/j.jmb.2005.06.076> PMID: 16055151
  79. Dawson A, Gibellini F, Sienkiewicz N, Tulloch LB, Fyfe PK, McLuskey K, et al. Structure and reactivity of *Trypanosoma brucei* pteridine reductase: Inhibition by the archetypal antifolate methotrexate. *Mol Microbiol.* 2006; 61: 1457–1468. <https://doi.org/10.1111/j.1365-2958.2006.05332.x> PMID: 16968221
  80. Mpamhanga CP, Spinks D, Tulloch LB, Shanks EJ, Robinson DA, Collie IT, et al. One Scaffold, Three Binding Modes: Novel and Selective Pteridine Reductase 1 Inhibitors Derived from Fragment Hits Discovered by Virtual Screening. *J Med Chem.* 2009; 52: 4454–4465. <https://doi.org/10.1021/jm900414x> PMID: 19527033
  81. Tulloch LB, Martini VP, Iulek J, Huggan JK, Lee JH, Gibson CL, et al. Structure-Based Design of Pteridine Reductase Inhibitors Targeting African Sleeping Sickness and the Leishmaniasis. *J Med Chem.* 2010; 53: 221–229. <https://doi.org/10.1021/jm901059x> PMID: 19916554
  82. Khalaf AI, Huggan JK, Suckling CJ, Gibson CL, Stewart K, Giordani F, et al. Structure-Based Design and Synthesis of Antiparasitic Pyrrolopyrimidines Targeting Pteridine Reductase 1. *J Med Chem.* 2014; 57: 6479–6494. <https://doi.org/10.1021/jm500483b> PMID: 25007262
  83. Zhao H, Bray T, Ouellette M, Zhao M, Ferre RA, Matthews D, et al. Structure of pteridine reductase (PTR1) from *Leishmania tarentolae*. *Acta Crystallogr Sect D Biol Crystallogr.* 2003; 59: 1539–1544. <https://doi.org/10.1107/S0907444903013131>
  84. Chang C-F, Bray T, Whiteley JM. Mutant PTR1 Proteins from *Leishmania tarentolae*: Comparative Kinetic Properties and Active-Site Labeling. *Arch Biochem Biophys.* 1999; 368: 161–171. <https://doi.org/10.1006/abbi.1999.1290> PMID: 10415124
  85. Hemsworth GR, Moroz O V, Fogg MJ, Scott B, Bosch-Navarrete C, Gonzalez-Pacanowska D, et al. The Crystal Structure of the *Leishmania major* Deoxyuridine Triphosphate Nucleotidohydrolase in Complex with Nucleotide Analogues, dUMP, and Deoxyuridine. *J Biol Chem.* 2011; 286: 16470–16481. <https://doi.org/10.1074/jbc.M111.224873> PMID: 21454646
  86. Bernier-Villamor V, Camacho A, Hidalgo-Zarco F, Pérez J, Ruiz-Pérez LM, González-Pacanowska D. Characterization of deoxyuridine 5'-triphosphate nucleotidohydrolase from *Trypanosoma cruzi* 1. *FEBS Lett.* 2002; 526: 147–150. [https://doi.org/10.1016/S0014-5793\(02\)03158-7](https://doi.org/10.1016/S0014-5793(02)03158-7) PMID: 12208522
  87. Nguyen C, Kasinathan G, Leal-Cortijo I, Musso-Buendia A, Kaiser M, Brun R, et al. Deoxyuridine Triphosphate Nucleotidohydrolase as a Potential Antiparasitic Drug Target. *J Med Chem.* 2005; 48: 5942–5954. <https://doi.org/10.1021/jm050111e> PMID: 16161998
  88. Björnberg O, Jordan DB, Palfey BA, Jensen KF. Dihydrooxonate is a substrate of dihydroorotate dehydrogenase (DHOD) providing evidence for involvement of cysteine and serine residues in base catalysis. *Arch Biochem Biophys.* 2001; 391: 286–94. <https://doi.org/10.1006/abbi.2001.2409> PMID: 11437361
  89. Cordeiro AT, Feliciano PR, Pinheiro MP, Nonato MC. Crystal structure of dihydroorotate dehydrogenase from *Leishmania major*. *Biochimie.* 2012; 94: 1739–1748. <https://doi.org/10.1016/j.biochi.2012.04.003> PMID: 22542640
  90. Inaoka DK, Sakamoto K, Shimizu H, Shiba T, Kurisu G, Nara T, et al. Structures of *Trypanosoma cruzi* dihydroorotate dehydrogenase complexed with substrates and products: Atomic resolution insights into mechanisms of dihydroorotate oxidation and fumarate reduction. *Biochemistry.* 2008; 47: 10881–10891. <https://doi.org/10.1021/bi800413r> PMID: 18808149
  91. Cardote TAF, Ciulli A. Cyclic and Macrocyclic Peptides as Chemical Tools To Recognise Protein Surfaces and Probe Protein-Protein Interactions. *ChemMedChem.* 2016; 11: 787–794. <https://doi.org/10.1002/cmdc.201500450> PMID: 26563831

92. Wiggers HJ, Rocha JR, Fernandes WB, Sesti-Costa R, Carneiro ZA, Cheleski J, et al. Non-peptidic Cruzain Inhibitors with Trypanocidal Activity Discovered by Virtual Screening and In Vitro Assay. *PLoS Negl Trop Dis*. 2013; 7: e2370. <https://doi.org/10.1371/journal.pntd.0002370> PMID: 23991231
93. Ndao M, Beaulieu C, Black WC, Isabel E, Vasquez-Camargo F, Nath-Chowdhury M, et al. Reversible cysteine protease inhibitors show promise for a Chagas disease cure. *Antimicrob Agents Chemother*. 2014; 58: 1167–78. <https://doi.org/10.1128/AAC.01855-13> PMID: 24323474
94. Jäger T, Koch O, Flohé L. Inhibition of Trypanothione Synthase as a Therapeutic Concept. Jäger T, Koch O, Flohé L, editors. *Trypanosomatid Diseases: Molecular Routes to Drug Discovery*. 2013: 429–443. <https://doi.org/10.1002/9783527670383.ch23>
95. Janin J, Miller S, Chothia C. Surface, subunit interfaces and interior of oligomeric proteins. *J Mol Biol*. 1988; 204: 155–164. [https://doi.org/10.1016/0022-2836\(88\)90606-7](https://doi.org/10.1016/0022-2836(88)90606-7) PMID: 3216390
96. Tsai C-J, Lin SL, Wolfson HJ, Nussinov R. Studies of protein-protein interfaces: A statistical analysis of the hydrophobic effect. *Protein Sci*. 1997; 6: 53–64. <https://doi.org/10.1002/pro.5560060106> PMID: 9007976
97. Glaser F, Steinberg DM, Vakser IA, Ben-Tal N. Residue frequencies and pairing preferences at protein-protein interfaces. *Proteins Struct Funct Genet*. 2001; 43: 89–102. [https://doi.org/10.1002/1097-0134\(20010501\)43:2<89::AID-PROT1021>3.0.CO;2-H](https://doi.org/10.1002/1097-0134(20010501)43:2<89::AID-PROT1021>3.0.CO;2-H) PMID: 11276079
98. Bogan AA, Thorn KS. Anatomy of hot spots in protein interfaces. *J Mol Biol*. 1998; 280: 1–9. <https://doi.org/10.1006/jmbi.1998.1843> PMID: 9653027